Journal of Porphyrins and Phthalocyanines
J. Porphyrins Phthalocyanines 2012; **16**: 1040–1054
DOI: 10.1142/S1088424612500769

Published at http://www.worldscinet.com/jpp/

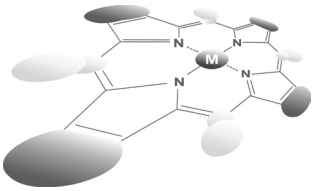

Use of chemical kinetics for the description of metal porphyrin reactivity

Tatyana N. Lomova[a◊], Mariya E. Klyueva[a,b], Elena Yu. Tyulyaeva*[a] and Nataliya G. Bichan[a]

[a] *G. A. Krestov Institute of the Solution Chemistry of Russian Academy of Sciences, Akademicheskaya str. 1, Ivanovo 153045, Russia*
[b] *Ivanovo State University of Chemistry and Technology, Engel's str. 7, Ivanovo 153000, Russia*

Received 20 January 2012
Accepted 16 March 2012

ABSTRACT: The results of use of chemical kinetics receptions, approaches and methods for the study of porphyrins and their metal complexes reactivity are discussed on an example of oxidation, acid-basic, and catalytic reactions of rhodium, palladium, and rhenium complexes of porphyrin in liquid solutions. The peculiarity of the porphyrin reaction rates is analyzed in a brief context of general provisions of the chemical kinetics. The opportunity to use the quasistationarity principle at the definition of the kinetic equation of the reactions with participation of metal porphyrins is shown. The transition from the process kinetic description to consideration of its mechanism is explored.

KEYWORDS: porphyrins, rhodium, palladium, rhenium complexes, synthesis, reactions, kinetics, mechanism.

INTRODUCTION

In spite of the fact that chemical kinetics methods are known rather for a long time they obviously are used in the chemistry of porphyrin compounds not enough. To certain extend this position connected with industrial-scale applications of porphyrins is developed poorly. Hence there are not necessary to make technological calculations of reactions using a kinetics equation. However chemical kinetics surely represents one of the most promising and exploited method for the study of mechanism of reactions. That allows writing a lot of equilibriums and completing stages independent from each other for a real not simple process and obtaining a limiting reaction rate [1]. Within the limits of phenomenological kinetics the change of concentration connected with physical processes in reacting system is not considered in the rate equation. It means that the equation describes only system consisting of elementary chemical reactions in total process in the closed reactor of periodic action [2].

A rate represents a barrier of course of chemical reaction. Spontaneous, from the point of view of thermodynamic criterion Gibbs free energy, reaction can proceed with too low speed to be appreciable in real conditions. This phenomenon concerns to the full of the reactions with participation of metal porphyrins because of their high stability and low reactivity in such reactions, as formation, oxidation, and dissociation. A chemical kinetics method gets special value for the study of such reactions. It is possible to describe reactivity quantitatively, having defined a rate constant with use of the method and to obtain the rate law — the kinetic equation, allowing to calculate the reaction rate at any concentration of reagents. Due to this possibility the method is a base for an optimization of synthesis and designing of porphyrin structures. Kinetic description and knowledge about elementary limiting reaction of chemical process are of great interest because of the possibility to regulate the rate of the reactions of metal porphyrins which are the potential components of the novel materials in catalyses and

◊SPP full member in good standing

*Correspondence to: Elena Yu. Tyulyaeva, email: teu@isc-ras.ru

electronics. In particular, the kinetic study shows a role of the chemically generated cation radicals of metal porphyrins as intermediates in the reactions catalyzed by these compounds.

Rare kinetics investigations in the field of porphyrin reactivity are reported every year [3–7]. However supramolecular assemblies [6], dendrite nanoprobes [4] or compounds with more complex structures [7–10] such as J-aggregates, Langmuir–Blodgett films and covalently linked tetrapyrrole macrocycles were studied and a rate of a photoinduced electron transfer or electron transport and electrocatalytic activity [4–7, 11] was determined without a full kinetic description of processes in most cases. In other works [12, 13] the progress of a reaction, as measured by the disappearance of the reagent, was monitored by UV-vis spectroscopy and by thin layer chromatography without a chemical kinetics method application. Our recent works have showed an ample opportunities of kinetic method for the study of structure-properties relationship [14–16] and for determining of elementary stages in a complex chemical process with a fractional, zero or negative reaction order with respect to a reagent [17].

The results of the kinetic description of acid-basic and oxidation reactions of palladium, rhodium, and rhenium complexes both with 5,10,15,20-tetraphenyl21H,23H-porphine and of 2,3,7,8,12,13,17,18-octaethyl21H,23H-porphin substituted at *meso*-positions with monophenyl, 5,15-diphenyl, 5,10-diphenyl, triphenyl, and tetraphenyl groups (complexes **1**–**9**) are presented in this work. The kinetics of the heterogenic catalytic reactions of H_2O_2 decomposition in a water-dimethylformamide-KOH system was studied as well. The role of palladium(II) porphyrin catalysts in a formation of elementary reactions, intermediate compounds, and kinetically significant equilibriums were determined.

EXPERIMENTAL

Complexes **1–7** were prepared [18, 19] by complexing of $PdCl_2$ solvated complex with the porphyrin ligand in dimethylformamide (DMFA). $Pd^{II}P$ **3–7** was synthesized by A. S. Semeikin at the Ivanovo State University of Chemical Technology. The spectral characteristics of the compounds were studied in this work or were obtained earlier [20].

(5,10,15,20-Tetraphenylporphinato)palladium(II) PdTPP, 1. The complex was prepared as described in [18]: H_2TPP and $PdCl_2$ in the molar ratio 1:10 were boiled in DMF until H_2TPP bands disappeared from the UV-vis spectrum of the reaction mixture. Then, the solvent was distilled *in vacuo*, the residue was dissolved in $CHCl_3$ and purified by repeated preparative chromatography on Al_2O_3 using $CHCl_3$. UV-vis ($CHCl_3$): λ_{max}, nm (log ε) 541 (3.92), 511 (4.11), 402 (4.84). IR (KBr): ν, cm^{-1} benzene ring vibrations, 696, 744 (γ C–H); 1071, 1075 (δ C–H); 1485, 1562, 1598 (ν C=C); 3040, 3054 (ν C–H); pyrrol ring vibrations, 791 (γ C–H); 1016 (C_3–C_4, ν C–N, δ C–H); 1312 (ν C–N); 1438 (ν C=N); 1540 (skeletal vibrations in pyrrol ring), 2853, 2973 (ν C–H); Pd–N –440, 470. ^1H NMR ($CDCl_3$): δ, ppm 8.81 (t, 8H, C_4H_2N, J = 3 Hz), 8.16 (t, 8H, *o*-Ph, J = 3 Hz), 7.75 (m, 8H, *m*-Ph, 4H, *p*-Ph).

(2,3,7,8,12,13,17,18-octaethylporphinato)-palladium(II) PdOEP, 2. The complex was prepared as described in [18]. UV-vis ($CHCl_3$): λ_{max}, nm (log ε) 545 (4.75), 511 (4.35), 392 (5.31). IR (KBr): ν, cm^{-1} pyrrol ring vibrations, 796 (γ C–H); 1317, 1305 (ν C–N); 1465, 1451 (ν C=N); 1554, 1602, 1632 (skeletal vibrations in

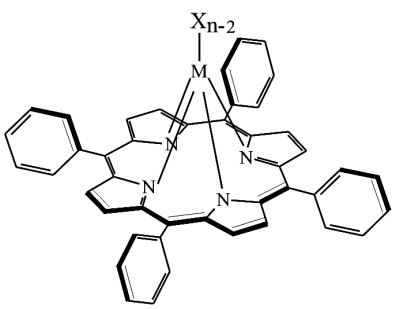

M = Pd, n = 2, PdTPP **1**

M = Rh, X = Cl, n = 3, (Cl)RhTPP, **8**

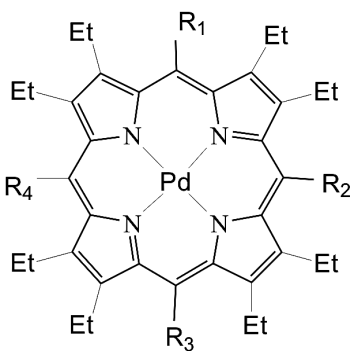

$R_1 = R_2 = R_3 = R_4$ = H, PdOEP, **2**

R_1 = Ph, $R_2 = R_3 = R_4$ = H, PdMPOEP, **3**

$R_1 = R_3$ = Ph, $R_2 = R_4$ = H, $Pd^{5,15}$DPOEP, **4**

$R_1 = R_2$ = Ph, $R_3 = R_4$ = H, $Pd^{5,10}$DPOEP, **5**

$R_1 = R_2 = R_3$ = Ph, R_4 = H, PdTriPOEP, **6**

$R_1 = R_2 = R_3 = R_4$ = Ph, PdTetPOEP, **7**

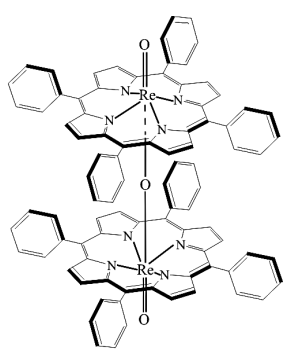

$[O=ReTPP]_2O$, **9**

pyrrol ring); ethyl vibrations, 837, 835 (γ C–H methine group); 1273 (δ C–H methine group), 2869, 2963 (ν CH_3); 2929 (ν CH_2); Pd–N -484. ^{1}H NMR ($CDCl_3$): δ, ppm 10.12 (s, 4H, *meso*), 4.08 (q, 16 H, CH_2), 1.92 (t, 24 H, CH_3).

(2,3,7,8,12,13,17,18-octaethyl-5-phenylporphinato)-palladium(II) PdMPOEP, 3. The synthesis was described in [19]. UV-vis ($CHCl_3$): λ_{max}, nm (log ε) 550 (4.59), 516 (4.34), 400 (5.50). IR (KBr): ν, cm^{-1} benzene ring vibrations, 710, 763 (γ C–H); 1088, 1167 (δ C–H); 1450, 1599 (ν C=C); 3020, 3057 (ν C–H); pyrrol ring vibrations, 781 (γ C–H); 1003 (C_3–C_4, ν C–N, δ C–H); 1317 (ν C–N); 1465 (ν C=N); 1500, 1631 (skeletal vibrations in pyrrol ring); ethyl vibrations, 840 (γ C–H methine group); 1259, 1278 (δ C–H methine group), 2870, 2963 (ν CH_3); 2929 (ν CH_2); Pd–N -486. ^{1}H NMR ($CDCl_3$): δ, ppm 10.10, 10.00 (d, d, 3H, *meso*), 8.17 (d, 2H, *o*-Ph), 7.63, 7.79 (t, m, 2H, *m*-Ph, H, *p*-Ph), 3.97, 2.65 (m, m, 16 H, CH_2), 1.91, 1.81, 1.12, 1.00 (m, m, t, t, 24 H, CH_3).

(2,3,7,8,12,13,17,18-octaethyl-5,15-diphenylporphinato)palladium(II) Pd^{5,15}DPOEP, 4. The synthesis was described in [19]. UV-vis ($CHCl_3$): λ_{max}, nm (log ε) 549 (4.47), 517 (4.28), 403 (5.25). IR (KBr): ν, cm^{-1} benzene ring vibrations, 705, 764 (γ C–H); 1091, 1173 (δ C–H); 1444, 1600 (ν C=C); 3020, 3056 (ν C–H); pyrrol ring vibrations, 784 (γ C–H); 1003 (C_3–C_4, ν C–N, δ C–H); 1317 (ν C–N); 1450, 1465 (ν C=N); 1498, 1632 (skeletal vibrations in pyrrol ring); ethyl vibrations, 842 (γ C–H methine group); 1261, 1279 (δ C–H methine group), 2870, 2963 (ν CH_3); 2929 (ν CH_2); Pd–N -486. ^{1}H NMR ($CDCl_3$): δ, ppm 9.79 (s, 2H, *meso*), 8.20 (d, 4H, *o*-Ph), 7.63, 7.79 (d, t, 4H, *m*-Ph, 2H, *p*-Ph), 3.90, 3.79, 2.54, 2.35 (q, q, q, q, 16 H, CH_2), 1.79, 1.64, 0.68, 0.60 (t, t, t, t, 24 H, CH_3).

(2,3,7,8,12,13,17,18-octaethyl-5,10-diphenylporphinato)palladium(II) Pd^{5,10}DPOEP, 5. The synthesis was described in [19]. UV-vis ($CHCl_3$): λ_{max}, nm (log ε) 561 (4.23), 527 (4.30), 412 (5.25). IR (KBr): ν, cm^{-1} benzene ring vibrations, 705, 758 (γ C–H); 1174 (δ C–H); 1443, 1599 (ν C=C); 3020, 3056 (ν C–H); pyrrol ring vibrations, 780, 794 (γ C–H); 1002 (C_3–C_4, ν C–N, δ C–H); 1314 (ν C–N); 1464 (ν C=N); 1501, 1632 (skeletal vibrations in pyrrol ring); ethyl vibrations, 839, 856, 880 (γ C–H methine group); 1261, 1286 (δ C–H methine group), 2870, 2964 (ν CH_3); 2929 (ν CH_2); Pd–N -484. ^{1}H NMR ($CDCl_3$): δ, ppm 9.98 (s, 2H, *meso*), 8.14 (d, 4H, *o*-Ph), 7.69, 7.62 (d, t, 4H, *m*-Ph, 2H, *p*-Ph), 3.88, 2.61 (q, q, 16 H, CH_2), 1.75, 0.98 (t, t, 24 H, CH_3).

(2,3,7,8,12,13.17,18-octaethyl-5,10,15-triphenylporphinato)palladium(II) PdTriPOEP, 6. The synthesis was described in [19]. UV-vis ($CHCl_3$): λ_{max}, nm (log ε) 570 (4.38), 536 (4.38), 422 (5.32). IR (KBr): ν, cm^{-1} benzene ring vibrations, 704, 761 (γ C–H); 1089, 1173 (δ C–H); 1443, 1598 (ν C=C); 3020, 3057 (ν C–H); pyrrol ring vibrations, 794 (γ C–H); 1003 (C_3–C_4, ν C–N, δ C–H); 1314 (ν C–N); 1465 (ν C=N); 1501, 1631 (skeletal vibrations in pyrrol ring); ethyl vibrations, 833, 844, 874 (γ C–H methine group); 1263, 1274 (δ C–H methine group), 2870, 2966 (ν CH_3); 2929 (ν CH_2); Pd–N -486. ^{1}H NMR ($CDCl_3$): δ, ppm 9.62 (d, H, *meso*); 8.21 (d, 8H, *o*-Ph), 7.71, 7.62 (d, t, 9H, *m*-Ph, 4H, *p*-Ph), 3.68, 2.52, 2.26 (q, q, q, 16 H, CH_2), 1.60, 0.65, 0.46 (t, t, t, 16 H, CH_3).

(2,3,7,8,12,13,17,18-octaethyl-5,10,15,20-tetraphenyl porphinato)palladium(II) PdTetPOEP, 7. The synthesis was described in [19]. UV-vis ($CHCl_3$): λ_{max}, nm (log ε) 580 (3.92), 544 (4.21), 433 (5.27). IR (KBr): ν, cm^{-1} benzene ring vibrations, 702, 760 (γ C–H); 1085 (δ C–H); 1443, 1598 (ν C=C); 3021, 3057 (ν C–H); pyrrol ring vibrations, 802 (γ C–H); 1003 (C_3–C_4, ν C–N, δ C–H); 1317, 1329 (ν C–N); 1462 (ν C=N); 1501, 1632 (skeletal vibrations in pyrrol ring); ethyl vibrations, 860, 879 (γ C–H methine group); 1261 (δ C–H methine group), 2870, 2969 (ν CH_3); 2929 (ν CH_2); Pd–N -486. ^{1}H NMR ($CDCl_3$): δ, ppm 8.22 (d, 8H, *o*-Ph, J = 4 Hz), 7.68 (m, 8H, *m*-Ph, 4H, *p*-Ph), 4.2 (d, 16 H, CH_2, J = 24 Hz), 2.4 (d, 16 H, CH_2, J = 23 Hz), 1.95 (d, 24 H, CH_3, J = 7 Hz), 0.5 (d, 24 H, CH_3, J = 7 Hz).

(5,10,15,20-tetraphenylporphinato)chlororhodium(III) (Cl)RhTPP, 8. H_2TPP was boiled with $RhCl_3$ in a mole ratio of 1:5 in PhCN until the bands of H_2TPP disappeared from the electronic absorption spectra of the reaction mixture. After the end of the reaction, the solvent was distilled in vacuum the reaction mixture was dissolved in chloroform and chromatographed twice on a column packed with Al_2O_3 (Brockmann activity grade II) using chloroform. UV-vis ($CHCl_3$): λ_{max}, nm (log ε) 569 (3.79), 535 (4.33), 421 (5.31). IR (KBr): ν, cm^{-1} phenyl substituents, 700, 749 (γ C–H); 1077, 1079 (δ C–H); 1489, 1533, 1575 (ν C=C); 3026, 3047 (ν C–H); pyrrole fragments, 788 (γ C–H); 1014 (C_3–C_4, ν C–N, δ C–H); 1349 (ν C–N); 1436 (ν C=N); 1540 (skeletal vibrations of pyrrole ring), 2827, 2907 (ν C–H); Rh–N -457, Rh–Cl –518, 549. ^{1}H NMR ($CDCl_3$): δ, ppm 8.93 (s, 8H, C_4H_2N, J = 3 Hz), 8.19 (d, 4H, *o*-Ph, J = 3 Hz), 8.34 (d, 4H, *o′*-Ph, J = 3 Hz), 7.76 (M, 8H, *m*-Ph, 4H, *p*-Ph).

μ-oxo-bis[(oxo)(5,10,15,20-tetraphenyl21H,23H-porphinato)]rhenium(V) [O=ReTPP]$_2$O, 9. The starting compound H_2ReCl_6 was prepared by reaction of ReO_2 with HCl under the heating. H_2TPP was boiled with H_2ReCl_6 in a mole ratio of 1:2 in PhOH until the bands of H_2TPP disappeared from the electronic absorption spectrum of the reaction mixture. After the end of the reaction, the solvent was cooled and the reaction mixture was extracted in chloroform, multiply washed with warm water to remove phenol and chromatographed on a column packed with Al_2O_3 (Brockmann activity grade II) using chloroform. Two zones were obtained: diluted green and concentrated green. Both zones were rechromatographed. Green compound was chromatographed on a column packed with silicagel using firstly benzene then mixed solution $CHCl_3$–C_2H_5OH as eluents. Three individual zones were separated: (1) orange (Cl)ReTPP (Fig. 1,

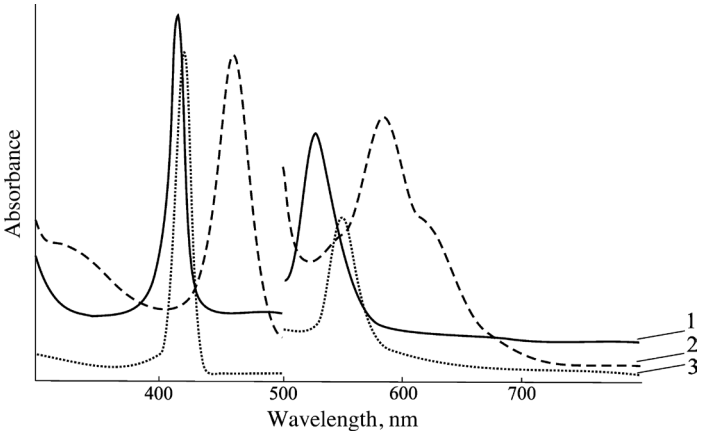

Fig. 1. UV-vis spectra in chloroform: (1) (Cl)ReTPP, (2) $[O=ReTPP]_2O$ and (3) (PhO)ReTPP

line *1*), (2) H_2TPP, and (3) green $[O=ReTPP]_2O$ (Fig. 1, line *2*). Greenish brown zone was chromatographed on a column packed with silicagel using firstly benzene then mixed solution $CHCl_3$–C_2H_5OH as eluents. Two individual zones were separated: (1) pink (PhO)ReTPP (Fig. 1, line *3*) and (2) green $[O=ReTPP]_2O$.

$[O=ReTPP]_2O$ yield — 75%. UV-vis ($CHCl_3$): λ_{max}, nm (log ε) 620 (sh), 582 (4.51), 461 (5.34), 333 (4.88). IR (solid chaotic layer): ν, cm^{-1} phenyl substituents, 702, 754 (γ C–H); 1072, 1179 (δ C–H); 1485, 1575, 1597 (ν C=C); 2954, 3056 (ν C–H); pyrrole fragments, 801 (γ C–H); 1018 (C_3–C_4, ν C–N, δ C–H); 1341 (ν C–N); 1440 (ν C=N); coordinating centre, 418 (Re–N); 568, 630, 854 (Re–O–Re); 961, 946 (Re=O). ^{1}H NMR ($CDCl_3$): δ, ppm 9.07 (d, 8H *o*-Ph, *J* = 7.6 Hz), 8.79 (s, 16H, C_4H_2N, *J* = 3 Hz), 8.01 (t, 8H *m*-Ph, *J* = 7.6 Hz), 7.60 (t, 8H *p*-Ph, *J* = 7.6 Hz), 7.47 (d, 8H *o′*-Ph, *J* = 7.6 Hz), 7.04, 6.87 (t, t, 8H *m′*-Ph, *J* = 7.6 Hz). ^{1}H NMR (D_2SO_4): δ, ppm 9.13 (m, 8H, C_4H_2N), 8.52, 8.23 (t, t, 8H *o*-Ph), 8.06 (t, 8H *m*-Ph, 4H *p*-Ph).

UV-vis spectra were recorded on an Agilent 8453 UV-vis, Specord M40, and SF-26 spectrophotometers. IR and ^{1}H NMR spectra were recorded on Specord M80 and AVANCE-500 (Bruker, tetramethylsilan as the internal standard), Bruker (200 MHz, hexamethyldisiloxane as the internal standard) spectrometers, respectively.

The kinetics of acid-basic and oxidation reactions of complexes **1**–**8** were studied spectrophotometrically. Solutions were thermostated in a cell installed in the spectrophotometer and heated with a U4 standard water thermostat. The error of temperature determination was ±0.1 K. The strength of aqueous sulfuric acid was determined by acid-base titration with an error within 0.15%.

The rates *W* of the decomposition of H_2O_2 of reagent grade in the presence of complexes **2–7** in the DMFA (chemically pure)–KOH (chemically pure)–H_2O (doubly distilled) system at 343–363 K and atmospheric pressure in a temperature-controlled reactor under continuous stirring conditions were determined volumetrically, by measuring the volume of oxygen released. An aqueous solution of H_2O_2 (18.1 ± 0.2 M) was added to a solution of a Pd complex and KOH in DMFA. The concentrations of complexes, KOH, and H_2O_2 were varied over the ranges 10^{-6}–10^{-4}, 0.0018–0.036, and 0.9–7.22 M, respectively. The *W* values were determined from the slope of the linear portion of the V_{O_2}–t dependence optimized by the method of least squares (Microsoft Excel) with respect to the positive direction of the abscissa axis. The activation parameters of the reaction *E* and $\Delta S^{\#}$ were determined from the temperature dependents of *W*.

The reaction complex formation between 5,10,15,20-tetraphenyl21H,23H-porphin and H_2ReCl_6 in boiling phenol was studied by means of investigating of intermediates and products structure with using of the spectral methods. The μ-oxo-dimer $[O=ReTPP]_2O$ dissociation reaction was studied by spectrophotometrical titration. The equilibrium constants were calculated using the equation (1), derived in accordance with the laws of mass action and the Bouguer–Lambert–Beer for a mixture of colored start compounds and products [1], where A_0, A_∞, and A_p are the absorbances of solutions of the starting metal porphyrin, reaction products, and their equilibrium mixture at the operating wavelength.

$$K = \frac{\dfrac{A_p - A_o}{A_\infty - A_o}}{1 - \dfrac{A_p - A_o}{A_\infty - A_o}} \cdot \frac{1}{\left(C_{AcOH} - C^o_{MP} \cdot \dfrac{A_p - A_o}{A_\infty - A_o}\right)^n} \qquad (1)$$

RESULTS AND DISCUSSIONS

Kinetics of oxidation reactions of rhodium(III) and palladium(II) porphyrins by aerated sulfuric acid

The porphyrin complexes **1**–**8** do not change at the time and at high temperatures in organic solvents and in AcOH and show the complex stability in liquid solutions. In medium containing sulfuric acid rhodium(III) and palladium(II) porphyrins undergo to irreversible transformation, which is apparent in evolution of UV-vis spectra (Fig. 2). The state and reactions of complexes **1**–**4**, **7** in concentrated aqueous sulfuric acid and of complexes **2**–**4**, **7** in mixed solutions AcOH–H_2SO_4 was studied quantitatively in [20]. The interaction between complex **8** and concentrated sulfuric acid was studied in this work.

The UV-vis spectra of complexes sharply change in strong acid. The spectra of compounds **1**, **7** and **8** (Fig. 2, the bottom line on the right part of figure) in concentrated H_2SO_4 contain two broad bands in the visible region with

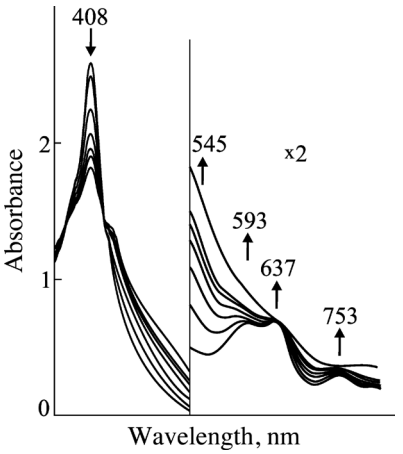

Fig. 2. The (Cl)RhTPP UV-vis spectrum changes in 16.52 M H_2SO_4 for 22000 at 323 K

λ_{max} of 538, 690 nm; 562, 710 nm, and 593 (sh), 637 (sh) accordingly because of the ion-molecule association of metalloporphyrin with the solvent proton (Equation (2), R is an acid anion or H_2O). Compounds **2** and **3** have analogous spectra in AcOH-H_2SO_4 with $C_{H_2SO_4}$ = 0.6–8.0 M.

$$PdP + H^+\ldots R \underset{}{\overset{K}{\rightleftharpoons}} PdP\ldots H^+\ldots R. \qquad (2)$$

Partial proton transfer from the solvent to the complex occurs at the C_{meso} atom of metalloporphyrins [21]. This interaction is not full proton transfer but the hydrogen bonding without aromatic system decomposition. High specific electron spectra of aromatic metal porphyrin H^+-associates were obtained for a lot of porphyrin complexes [21]. The rhodium(III) and palladium(II) complexes studied in this work, accordingly with their chloro-ligand and $4d^8$ electronic configuration, satisfy the conditions required for association with proton in strong acid media containing sulfuric acid — the presence an electron donor ligand or an Pd–N dative π component in the coordination interaction and in both cases — the absence electron–acceptor substituents in the macrocycle and phenyl rings [21]. In mixed solutions AcOH–H_2SO_4 weak acid media two electron–acceptor phenyl substituents (complex **4**) are enough in order to H^+-associate formation was not probably.

Spectral study of the complexes **2**–**4** at 298 K and **1**, **7** and **8** at high temperatures showed that the reaction product in concentrated H_2SO_4 for both group of complexes is the precursor complex oxidized in the aromatic macrocycle (the π-cation radical $PdP^{+\bullet}$). This complex form is identified by the characteristic wide-band electronic spectrum between 500 and 700 nm and the band with a peak at ≈ 750 nm (Fig. 2, the top line on the right part of figure). This UV-vis spectrum was obtained for the product of one electron chemical oxidation of PdTPP in CH_2Cl_2 [22]. The transition of the precursor complex into its π-cation radical $PdP^{+\bullet}$ (Equations 3 and 4) is observed for complexes **1, 7,** and **8** in the course of the transformation indicating by the existence of an isosbestic point between bands at 408 and 545 nm in the set of spectral curves (Fig. 2). For the palladium complex with H_2TetPOEP its oxidized species was isolated in an unchanged state (with HSO_4^- as opposite ion) by reprecipitation from sulfuric acid.

$$PdP\ldots H^+\ldots R + O_2 + H^+ \rightarrow PdP^{+\bullet} + HO_2^{\bullet} + H^+\ldots R \qquad (3)$$

$$(Cl)RhTPP\ldots H^+\ldots R + O_2 + H^+ \rightarrow (Cl)RhTPP^{+\bullet} + HO_2^{\bullet} + H^+\ldots R \qquad (4)$$

Analogous process (Equation 3) takes place in the case of complexes **2**–**4** in mixed solutions AcOH–H_2SO_4 with $C_{H_2SO_4}$ = 0.6–8.0 M at 333–363 K and of complex **7** in AcOH – 0.1–1.0 M H_2SO_4 at 298 K. However, the complex **4** react in molecular form and complex **7** undergo oxidation in solvating process.

Kinetic data presented on Tables 1 and 2, and Figs 2–4 are described by the third-order or second-order rate equations (5–8) obtained within the limits of phenomenological kinetics. The left part of these equations is an experimental rate of a complex process that is proportional with a reacted compounds concentration in a corresponding degrees (n) determined experimentaly. At the first the order with respect to metal porphyrin with controlled concentrations was examined. One is equal 1 according to data of Tables 1 and 2. At the second the orders with respect to acid particles of the solvent were obtained by the extra concentrations method — due to a relation $\log k_{obs}$ *vs.* $\log C^0_{H_2SO_4}$ (in AcOH or in H_2O) with the slope ratio equal to the reaction order n (Figs 3 and 4). One allowed to determine the rate constants for the reactions (3 and 4), named a kinetic coefficient in a case of the complex reactions (Table 3), and to discuss the elementary reactions in the transformations of metal porphyrin complexes after obtaining the additional data about reactions (no reversibility, a product nature, oxygen absence influence).

The rate low for complexes **1** and **7** in concentrating sulfuric acid is:

$$-dC_{PdP}/d\tau = k \times C_{PdP} \times [H_2SO_4]^2, \qquad (5)$$

for complexes **2** and **3** in AcOH–H_2SO_4

$$-dC_{PdP}/d\tau = k \times C_{PdP} \times (C^0_{H_2SO_4})^2 \qquad (6)$$

for complex **4** in AcOH–H_2SO_4

$$-dC_{Pd^{5,15}DPOEP}/d\tau = k \times C_{Pd^{5,15}DPOEP} \times C^0_{H_2SO_4} \qquad (7)$$

The rate low for complex **8** in concentrating sulfuric acid analogues to Equation (5) is:

$$dC_{(Cl)RhTPP}/d\tau = k \times C_{(Cl)RhTPP} \times [H_2SO_4]^2 \qquad (8)$$

Here $[H_2SO_4]$ and $C^0_{H_2SO_4}$ are equilibrium and initial sulfuric acid concentration. Table 3 lists the rate constants and activation parameters for the reactions of PdTPP and PdTetPOEP with H_2SO_4 found in the course

Table 1. Effective kinetic parameters[a] of the oxidation reaction of PdMPOEP or Pd[5,15]DPOEP in mixed solutions AcOH–H_2SO_4

$c^{o}_{H_2SO_4}$, M	T, K	$k_{obs} \times 10^5$, s^{-1}	E_{obs}, kJ.mol^{-1}	$-\Delta S^{\#}_{obs}$, J.mol^{-1}.K^{-1}
PdMPOEP				
	348	1.60 ± 0.15		
2.79	353	2.3 ± 0.2	81 ± 4	111 ± 13
	358	3.5 ± 0.3		
	348	2.0 ± 0.2		
3.22	353	2.8 ± 0.2	79 ± 6	115 ± 20
	358	4.28 ± 0.40		
	348	2.7 ± 0.1		
3.65	353	3.8 ± 0.3	75 ± 4	124 ± 13
	358	5.6 ± 0.7		
	348	3.3 ± 0.2		
4.07	353	4.7 ± 0.3	75 ± 2	124 ± 7
	358	6.85 ± 0.60		
4.50	348	3.9 ± 0.3	68	141
	353	5.4 ± 0.3		
Pd[5,15]DPOEP				
	333	1.63 ± 0.10		
2.40	338	1.93 ± 0.15	28 ± 4	260 ± 13
	343	2.18 ± 0.20		
	333	2.12 ± 0.20		
3.08	338	2.5 ± 0.15	27 ± 3	260 ± 10
	343	2.8 ± 0.2		
	333	2.54 ± 0.24		
3.43	338	2.95 ± 0.20	27 ± 1	259 ± 3
	343	3.4 ± 0.3		
	333	3.15 ± 0.20		
4.11	338	3.60 ± 0.2	23 ± 2	269 ± 7
	343	4.03 ± 0.35		

[a] Observed rate constant (k_{obs}), activation energy (E_{obs}) and activation entropy ($-\Delta S^{\#}_{obs}$) calculated from log k–1/T plot.

of the least-squares fit ($\log k^{T}_{obs}$ *vs*. log [H_2SO_4]). The presentation in log k^{T}_{obs}–log[H_2SO_4] coordinates uses the H_2SO_4 equilibrium concentration in strong aqueous sulfuric acid; therefore, H_2SO_4 ionization preequilibrium has already been included into Equation (5).

The rate lows (5–8) are analogous to dissociation reactions of some metal porphyrin coordination centre. However the transformations of rhodium and palladium complexes in H_2SO_4 are not the reaction leading up to complex dissociation. The proton of the H^+-associated complex species is not involved in the dissociation of porphyrin complexes [24, 25]. Other mechanisms operate in the transformations of investigating complexes in H_2SO_4 (Equations 9, 10); rate Equation (5) can only be interpreted on the assumption that the associated proton (Equation 2) is involved in the reaction and R = HSO_4^-:

$$PdP\ldots H^+\ldots R + O_2 \rightarrow (O_2)PdP + H^+\ldots R, \text{ fast} \quad (9)$$

$$(O_2)PdP + H_2SO_4 \rightarrow PdP^{+\bullet} + HO_2^{\bullet} + HSO_4^-, \text{ slow} \quad (10)$$

Writing rate equation for slow reaction (10) with $C_{(O_2)PdP}$ equal to $C_{PdP\ldots H^+\ldots R}$, so $K \times C_{PdP} \times C_{H^+\ldots R}$ (K is equilibrium constant of H^+-associate formation (2)) give the third-order rate Equation (5) in which $k = k_{slow}$ K. Thus, PdTPP and PdTetPOEP in strong sulfuric acid experience multistage oxidation. Kinetically significant

Table 2. Effective kinetic parameters[a] of the oxidation reaction of PdTetPOEP in concentrated H_2SO_4

$C^{o}_{H_2SO_4}$, M	$[H_2SO_4]$[b], M	T, K	$k_{obs} \times 10^4$, s^{-1}	E_{obs}, kJ.mol^{-1}	$-\Delta S^{\#}_{obs}$, J.mol^{-1}.K^{-1}
17.48	11.096	298	$(1.4 \pm 0.5)\cdot10^{-3}$	104 ± 4	32 ± 12
	11.646	343	0.53 ± 0.02		
	11.630	353	1.40 ± 0.03		
	11.606	358	2.35 ± 0.10		
	11.573	363	4.0 ± 0.1		
17.74	12.406	298	$(2.1 \pm 0.4)\cdot10^{-3}$	103 ± 5	33 ± 15
	12.875	343	0.64 ± 0.02		
	12.836	353	1.64 ± 0.05		
	12.803	358	2.8 ± 0.1		
	12.760	363	4.7 ± 0.2		
17.86	12.504	298	$(2.8 \pm 0.6)\cdot10^{-3}$	104 ± 3	30 ± 9
	13.462	343	0.68 ± 0.01		
	13.414	353	1.89 ± 0.06		
	13.376	358	3.1 ± 0.1		
	13.330	363	5.1 ± 0.1		
18.03	13.753	298	$(4 \pm 1)\cdot10^{-3}$	102 ± 3	35 ± 9
	14.084	343	0.77 ± 0.01		
	14.028	353	2.17 ± 0.06		
	13.987	358	3.4 ± 0.2		
	13.938	363	5.4 ± 0.2		
18.23	14.551	298	$(4.4 \pm 0.9)\cdot10^{-3}$	102 ± 2	33 ± 6
	15.208	343	0.92 ± 0.02		
	15.151	353	2.45 ± 0.10		
	15.106	358	4.10 ± 0.15		
	15.053	363	6.6 ± 0.2		

[a]Observed rate constant (k_{obs}), activation energy (E_{obs}) and activation entropy ($-\Delta S^{\#}_{obs}$) calculated from $\log k$–$1/T$ plot; [b]equilibrium sulfuric acid concentration from [23].

are the rate-controlling stage of one-electron oxidation of metalloporphyrin by coordinated dioxygen with the help of H^+ and partial protonation of the macrocyclic complex (Equation 2).

The oxidation reaction, for complexes **2** and **3** in AcOH–H_2SO_4 analogous with reaction (3), for complex **4** is:

$$PdP + O_2 + H^+ \rightarrow PdP^{+\bullet} + HO_2^{\bullet} \qquad (11)$$

The scheme of the plain reactions for this case is: two preequilibriums and slow reaction of one-electronic oxidation

$$H_2SO_4 + AcOH \leftrightarrow AcOH_2^+ + HSO_4^-;$$
$$K_a = [AcOH_2^+] \times [HSO_4^-]/[H_2SO_4] \qquad (12)$$

$$PdP + O_2 \leftrightarrow (O_2)PdP \qquad (13)$$

$$(O_2)PdP + H_2SO_4 \rightarrow PdP^{+\bullet} + HO_2^{\bullet} + HSO_4^-, \text{ slow} \qquad (14)$$

pK_a = 4.3 or 4.5 according to [26] and [27]. The equilibrium (13) is displaced probably to the right because of the big surplus of oxygen in comparison with PdP. It is obvious, that coordination of molecule O_2 on the Equation (13) is accompanied by destruction H-associate PdP…H^+…R in reaction of complexes **2** and **3**. Slow reaction (14) passes at action of H_2SO_4 molecules, as acid particle with the highest concentration in the reaction mixture.

The rate equation can be written down in view of equality $C^0_{H_2SO_4}$ = $[H_2SO_4]$ + $[AcOH_2^+]$ and $[H_2SO_4]$ ~ $C^0_{H_2SO_4}$ (because of the small value of pK_a) by the Equations (15) and (16) for complexes **2**, **3** and for complex **4** correspondently. The first equality have been written in view of equilibrium (13) — how many molecules of (O_2)PdP have reacted in (14) during $d\tau$, so much these have obtained (so much PdP molecules have reacted) according to (13) [1]. The second equality is a mathematical expression of the law of mass action

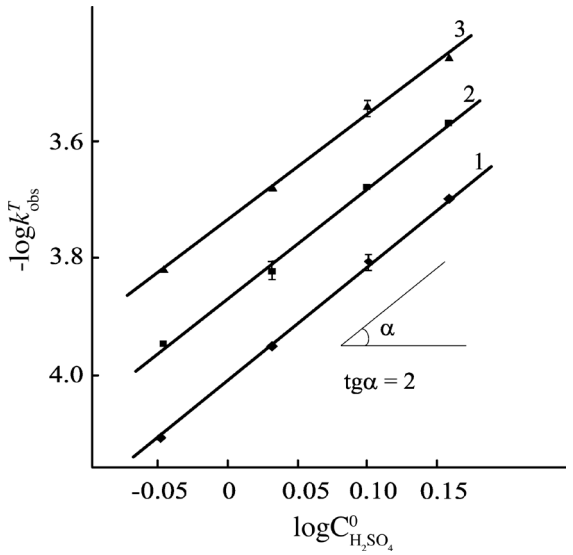

Fig. 3. Dependence of observed rate constant ($\log k^T_{obs}$) on the initial concentration of H_2SO_4 ($\log C^0_{H_2SO_4}$) for PdOEP in AcOH–H_2SO_4 with $\log C^0_{H_2SO_4}$ = 0.9 ÷ 1.4 M at temperatures (1) 353, (2) 358, (3) 363 K. R^2 = 0.98 ÷ 0.99

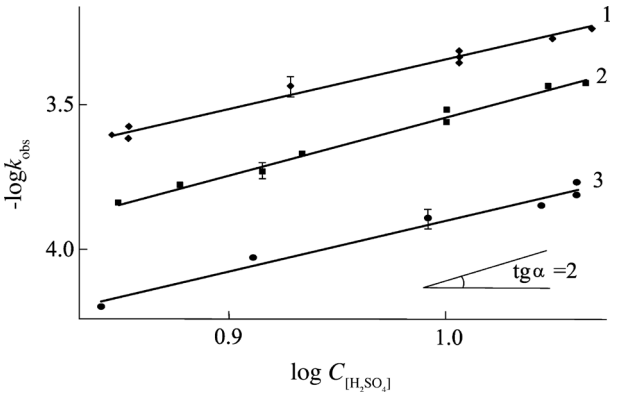

Fig. 4. Dependence of observed rate constant ($\log k_{obs}$) on equilibrium concentration of H_2SO_4 ($\log C_{[H_2SO_4]}$) for the reaction of (Cl)RhTTP in H_2SO_4 at temperatures (1) 328, (2) 323, and (3) 318 K. R^2 are equal 0.98, 0.99, and 0.98, respectively

[1] for limiting elementary reaction (14). In next the equalities $C_{(O_2)PdP}$ and $[H_2SO_4]$ are expressed according to equilibrium transformations (12) and (13).

$$\begin{aligned} -dC_{PdP}/d\tau &= -dC_{(O_2)PdP}/d\tau \\ &= k_{slow} \times C_{(O_2)PdP} \times [H_2SO_4] \\ &= k_{slow} \times K^{-1}_a \times K \times C_{PdP} \times C_{H^+\ldots R} \times [H_2SO_4] \\ &= k_{slow} \times K^{-1}_a \times K \times C_{PdP} \times (C^0_{H_2SO_4})^2 \end{aligned} \quad (15)$$

$$\begin{aligned} -dC_{Pd^{5,15}DPOEP}/d\tau &= -dC_{(O_2)Pd^{5,15}DPOEP}/d\tau \\ &= k_{slow} \times C_{(O_2)\,Pd^{5,15}DPOEP} \times [H_2SO_4] \\ &= k_{slow} \times C_{Pd^{5,15}DPOEP} \times C^0_{H_2SO_4} \end{aligned} \quad (16)$$

The high stability of (Cl)RhTPP and PdP towards acids and oxidation of their aromatic part are caused by the strong $\sigma\pi$-bonding of the central atom. According to obtained data these aromatic complexes are stable toward coordination center dissociation because of easy π-cation-radical formation. The modification of *meso*-positions of coordinating ligand can be considered as a way of change of electron donating properties of the complexes important in oxidation reactions and partial carry of a proton from the medium.

Alkaline decomposition of hydrogen peroxide in a water-dimethylformamide medium catalyzed by palladium(II) porphyrins

The kinetic and spectral description of alkaline decomposition of H_2O_2 in a water-dimethylformamide medium catalyzed by $Pd^{II}P$ (complexes 2–7) is an example of successful research of the chemical reaction route (stoicheometric mechanism).

Table 3. Kinetic parameters of the oxidation reaction of PdOEP, PdMPOEP, $Pd^{5,15}$DPOEP in mixed solutions AcOH–H_2SO_4 and PdTPP, PdTetPOEP and (Cl)RhTPP in concentrated H_2SO_4

T, K	$k^a \times 10^6$, $M^{-2}.s^{-1}$	$E^{a,b}$, kJ.mol^{-1}	$-\Delta S^{\#\,a,b}$, J.mol^{-1}.K^{-1}
PdTPP			
343	1.05 ± 0.16	60 ± 5	195 ± 20
348	1.5 ± 0.2		
353	1.9 ± 0.2		
298[a]	$4.6 \cdot 10^{-2}$		
PdTetPOEP			
343	0.39 ± 0.01	104 ± 3	70 ± 10
353	1.05 ± 0.03		
358	1.74 ± 0.03		
363	2.87 ± 0.04		
298[b]	$1.83 \cdot 10^{-3}$		
PdOEP			
298[b]	1.15	70 ± 1	131 ± 3
353	100		
358	138		
363	191		
PdMPOEP			
298[b]	0.008	91 ± 7	102 ± 23
348	2.2		
353	3.3		
358	5.3		
$PdD^{5,15}POEP$			
298[b]	1.2[c]	33 ± 5	254 ± 16
333	5.5[c]		
338	6.8[c]		
343	7.8[c]		
(Cl)RhTPP			
298	0.4[d]	120[d]	−17[d]
318	2.0		
323	2.5		
328	8.0		

[a]Kinetic coefficient (*k*) in Equations (5–8), activation energy (*E*) and activation entropy ($-\Delta S^{\#}$); [b]found by extrapolation of the $\log k$–$1/T$ plot; [c]$M^{-1}.s^{-1}$; [d]are represented rough values because of appreciable differences of the reaction order at various temperatures from exact value *n* = 2 (Equation 8).

Table 4. Rate of H_2O_2 decomposition (W) catalyzed by palladium(II) porphyrins at various alkaline (KOH) and hydrogen peroxide (H_2O_2) concentrations at T = 343 K

Complex	C_{KOH}, M	W^a, $mL_{O_2}.min^{-1}$	$C^o_{H_2SO_4}$, M	W^b, $mL_{d_2}.min^{-1}$
PdOEP	0.0018	0.37 ± 0.02	0.902	0.30 ± 0.02
	0.018	2.20 ± 0.17	1.805	0.60 ± 0.03
	0.036	3.58 ± 0.16	3.61	2.20 ± 0.17
			5.415	4.62 ± 0.17
			7.22	7.78 ± 0.25
PdMPOEP			0.902	0.30 ± 0.03
			1.805	0.60 ± 0.02
			3.61	1.59 ± 0.09
			5.415	3.19 ± 0.08
			7.22	6.99 ± 0.23
$Pd^{5,15}$DPOEP	0.018	1.53 ± 0.14		
		1.56 ± 0.11		
		1.82 ± 0.14		
$Pd^{5,10}$DPOEP			0.902	0.40 ± 0.05
			1.805	0.75 ± 0.06
			3.61	1.51 ± 0.06
			5.415	3.28 ± 0.13
			7.22	6.43 ± 0.15
PdTriPOEP	0.0018	0.42 ± 0.01		
	0.018	1.40 ± 0.09		
	0.036	2.76 ± 0.07		
PdTetPOEP			0.902	0.50 ± 0.04
			1.805	0.80 ± 0.05
			3.61	1.63 ± 0.07
			5.415	3.66 ± 0.12
			7.22	6.96 ± 0.25

[a] $C_{H_2O_2}$ = 3.61 M, $C_{PdP} \cdot 10^5$, M: 2.15, 2.80, and 0.34, 3.40, 13.6 for PdOEP, PdTriPOEP, and $Pd^{5,10}$DPOEP, [b] $C_{PdP} \cdot 10^5$, M: 2.15, 2.82, 2.90, and 2.10 for PdOEP, PdMPOEP, $Pd^{5,10}$DPOEP, and PdTetPOEP.

Decomposition process was studied over a wide range of reagent concentrations. The results of the study of PdP catalytic activity are presented in Table 4 and Figs 5 and 6. These data show that W increases with growing of the concentrations of KOH and H_2O_2. In all cases, there is a satisfactory linear correlation between the logarithm of W and the concentration of KOH with a slope close to one. It is found that log$W$ linearly depends from log$C_{H_2O_2}$ in two regions of H_2O_2 concentrations, 0.9–3.6 and 3.6–7.2 M H_2O_2 (Fig. 6). The order of the reaction in $C_{H_2O_2}$ is close to 1 and 2, respectively. At last the reaction order with respect to the concentration of the catalysts is close to zero because the rate W is almost independent of C_{PdP}. Zero reaction order with respect to PdP is evidence of a heterogeneous catalytic process.

Named results are in line with the total second-order and third-order kinetic equations for the ranges $C_{H_2O_2}$ = 0.9–3.6 and 3.6–7.2 M:

$$dC_{O_2}/d\tau = k \times (C_{PdP})^0 \times C_{H_2O_2} \times C_{KOH} \times (C_{O_2})^0 = k \times C_{H_2O_2} \times C_{KOH} \quad (17)$$

$$dC_{O_2}/d\tau = k' \times (C_{PdP})^0 \times (C_{H_2O_2})^2 \times C_{KOH} \times (C_{O_2})^0 = k' \times (C_{H_2O_2})^2 \times C_{KOH} \quad (18)$$

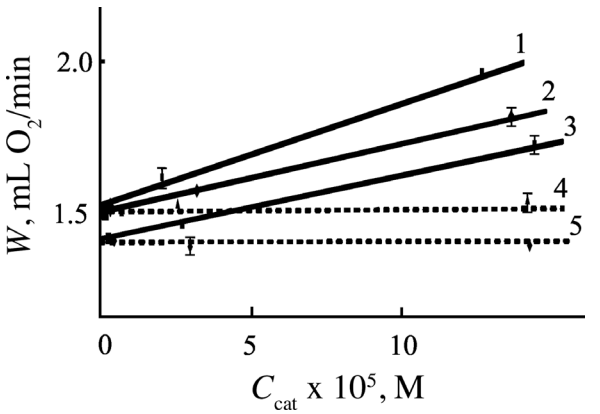

Fig. 5. Dependences of the rate of H_2O_2 decomposition (W) on the concentration of catalyst (C_{cat}) (1) PdTetPOEP, (2) $Pd^{5,15}$DPOEP, (3) $Pd^{5,10}$DPOEP, (4) PdMPOEP, (5) PdTriPOEP at H_2O_2 concentration 3.61 M and KOH concentration 0.018 M at temperature 343 K

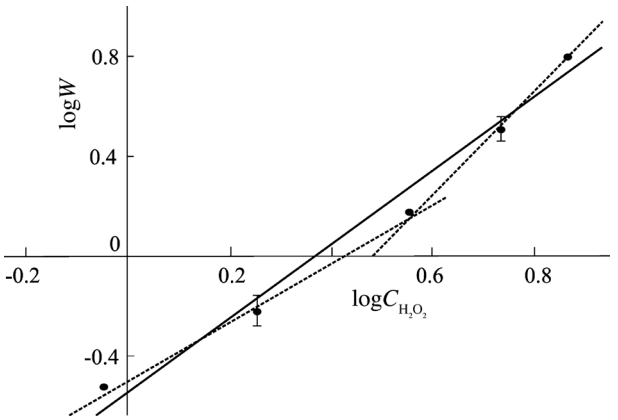

Fig. 6. Dependences of the rate of H_2O_2 decomposition ($\lg W$) on the H_2O_2 concentration ($\lg C_{H_2O_2}$) in the presence of catalyst PdMPOEP with concentration 2.82×10^{-5} M and KOH concentration 0.018 M at temperature 343 K. R^2 = 0.995 and 0.999 to left and to right broken lines, R^2 = 0.992 to solid line

Table 5. Rate constants of H_2O_2 decomposition[a] catalyzed by palladium(II) porphyrins at 343 K

Complex	k', $mL_{O_2}.l^2.mol^{-1}.min^{-1}$	k'', $mL_{O_2}.l^3.min^{-1}.mol^{-3}$
PdOEP	14.5 ± 1.8	4.5 ± 0.9
PdMPOEP	18.1	5.07
Pd[5,10]DPOEP	24.3	5.7
PdTetPOEP	29.2	6.2

[a]Kinetic coefficients in Equation (17) (k) and (18) (k'), respectively.

The main rate constants k and k' for PdP at T = 343 K were found by optimizing of the $\log W$–$C_{H_2O_2}$ dependence (complexes **3**, **5**, **7**) or from two values for each constant determined in two independent experiments by optimizing of the same dependence and the $\log W$-$\log C_{KOH}$ dependence (complex **2**) (Table 5).

In the electronic absorption spectra of freshly prepared mixtures PdP–DMFA–H_2O–KOH, when gas release is insignificant and there is no precipitate, the $Q(0, 0)$ and $Q(0, 1)$ absorption bands of the initial PdP complexes in DMFA with maxima at 508–545 and 540–581 nm, respectively (Fig. 7a), experience broadening and bathochromic shifts by 3–23 nm (Fig. 7b). An increase in overall absorption background and the appearance of absorption in the longwave region and visible spectrum region adjacent to the UV range are observed. Such electronic absorption spectra are characteristic of π radical cation forms of metalloporphyrins obtained by chemical and electrochemical oxidation [27, 28]. After gas release terminates, complexes from a solution of **2**, **3** and **4** heterogeneous systems were isolated into $CHCl_3$, and these solutions were thoroughly washed from DMFA, KOH, and H_2O_2. The electronic absorption spectra of solutions in chloroform contained bands of initial PdP. Changes in the spectra of PdP in the PdP–DMFA–H_2O–KOH–H_2O_2 system compared with its solution in DMFA can therefore be explained by the formation of π radical cation forms $PdP^{+\bullet}$.

The elementary reactions in the complex transformations of H_2O_2 (Equation 19) showed on the Scheme 1 explain the kinetic Equations (17) and (18).

$$2H_2O_2 \rightarrow H_2O + O_2 \qquad (19)$$

In order to maintain the nature of k and k' we can use the relations like in the case of kinetics of rhodium(III) and palladium(II) porphyrins oxidation reactions. A rate low for limiting stages we will write in view of fast irreversible reactions and previous equilibrium (Scheme 1). The kinetic equations of slow stages (20, 21) in the scheme are written as Equations (22) and (23).

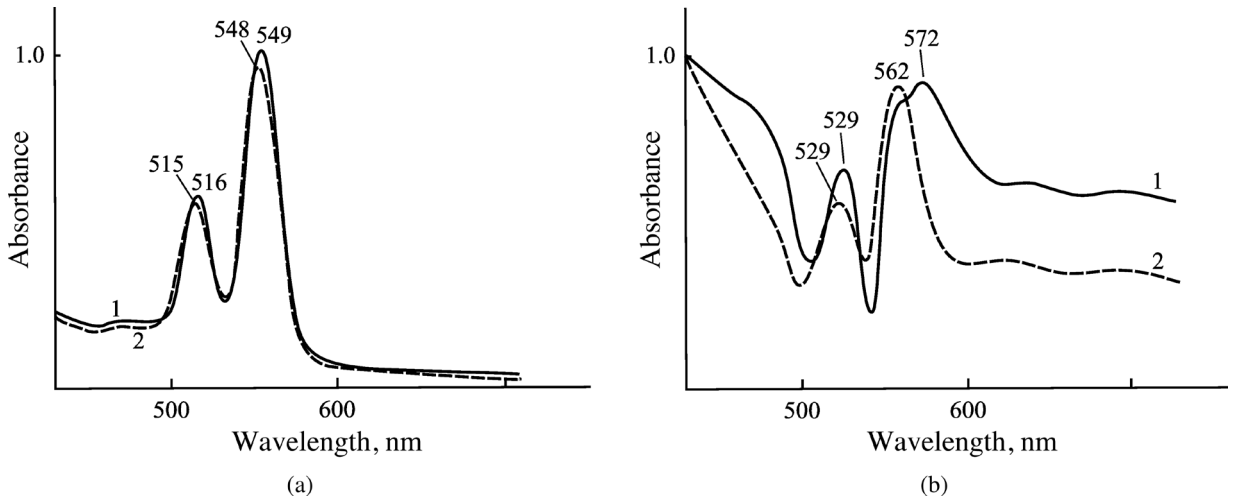

Fig. 7. UV-vis spectra of (1) PdMPOEP and (2) Pd[5,15]DPOEP in (a) DMFA and (b) DMFA–H_2O–KOH–H_2O_2 mixture with H_2O_2 concentration 3.61 M and KOH concentration 0.018 M at temperature 298 K

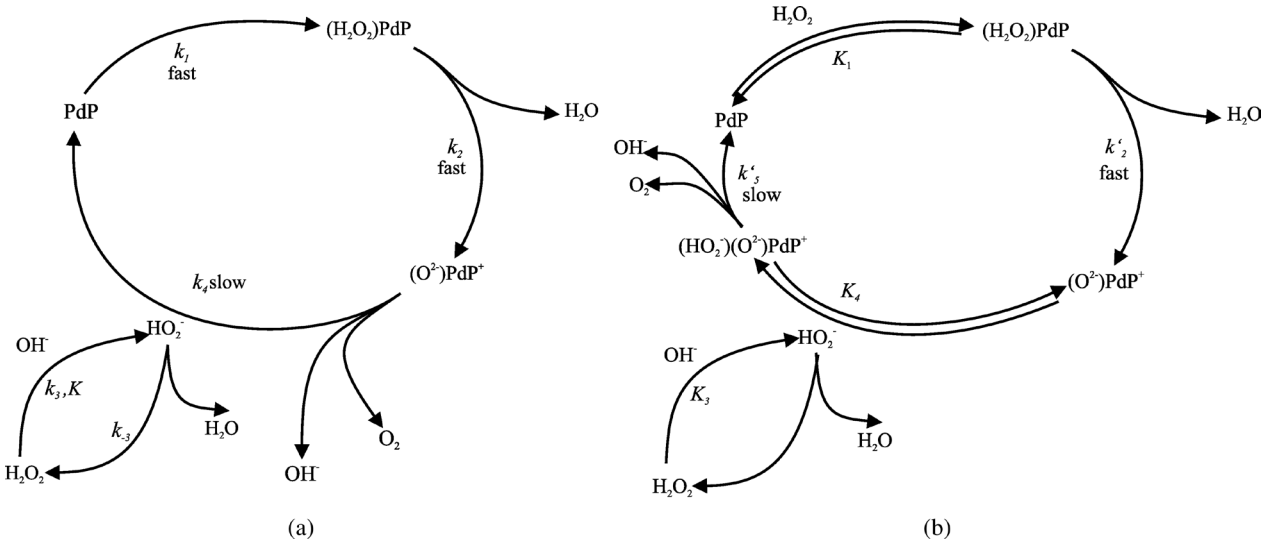

Scheme 1. The transformations in PdP–DMFA–H_2O–KOH–H_2O_2 system for the intervals (a) $C_{H_2O_2}$ = 0.9–3.6 M and (b) $C_{H_2O_2}$ = 3.6–7.2 M

$$(O^{2-})PdP^{+\bullet} + HO_2^- \xrightarrow{k_4} PdP + OH^- + O_2, \text{ slow} \quad (20)$$

$$(HO_2^-)(O^{2-})PdP^{+\bullet} \xrightarrow{k'_5} PdP + OH^- + O_2, \text{ slow} \quad (21)$$

$$\begin{aligned} -dC_{HO_2^-}/d\tau &= dC_{O_2}/d\tau \\ &= k_4 \times C_{(O^{2-})PdP^{+\bullet}} \times C_{HO_2^-} \\ &= k_4 \times K \times C_{PdP} \times C_{H_2O_2} \times C_{OH^-} \end{aligned} \quad (22)$$

$$\begin{aligned} -dC_{(HO_2^-)(O^{2-})PdP^{+\bullet}}/d\tau &= dC_{O_2}/d\tau \\ &= k'_5 \times C_{(HO_2^-)(O^{2-})PdP^{+\bullet}} \end{aligned} \quad (23)$$

Equation (22) for limiting stage on Scheme 1a is identical to experimental Equation (17). It is possible to write down following equality

$$C_{(HO_2^-)(O^{2-})PdP^{+\bullet}} = K_4 \times C_{(O^{2-})PdP^{+\bullet}} \times C_{HO_2^-} \quad (24)$$

$$C_{HO_2^-} = K_3 \times C_{H_2O_2} \times C_{OH^-} \quad (25)$$

$$\begin{aligned} C_{(O^{2-})PdP^{+\bullet}} &= C_{(H_2O_2)PdP}, C_{(H_2O_2)PdP} \\ &= K_1 \times C_{PdP} \times C_{H_2O_2} \end{aligned} \quad (26)$$

$$C_{(HO_2)(O^{2-})PdP^{+\bullet}} = K_4 \times K_1 \times K_3 \times C_{PdP} \times (C_{H_2O_2})^2 \times C_{OH^-} \quad (27)$$

$$dC_{O_2}/d\tau = k_5 \times K_4 \times K_1 \times K_3 \times C_{PdP} \times (C_{H_2O_2})^2 \times C_{OH^-} \quad (28)$$

Equation (23) for limiting stage on Scheme 1b is identical to experimental Equation (18). Thus kinetic coefficients k and k' include the thermodynamic constants of kinetic significant equilibriums:

$$k = k_4 \times K \quad (29)$$

$$k' = k_5 \times K_1 \times K_3 \times K_4 \quad (30)$$

Thus catalysis with PdP follows a more complex scheme than simple decomposition of H_2O_2 in an alkaline medium. At the initial stages (before the radical-ion mechanism begins to operate), we have a quasi-equilibrium system with acid-base catalysis [29],

$$H_2O_2 + OH^- \leftrightarrow HO_2^- + H^+ \quad (31)$$

$$2HO_2^- \rightarrow 2OH^- + O_2 \quad (32)$$

According to [29], the rate of such a reaction increases up to the complete shift of equilibrium (31) to the right and then decreases. In experiments with PdP, the concentration of OH^- is much lower than $C_{H_2O_2}$ (Table 4), and the rate of the decomposition of H_2O_2 increases for all PdP as grows; that is, all the experiments were performed in the region preceding maximum rate rise. Within the first range of concentrations, the PdP–H_2O_2–KOH system (Scheme 1a) does indeed work as a quasi-equilibrium system. The coordination of the second peroxide molecule (in the form of HO_2^-), which is a slow and irreversible reaction at low concentrations (Scheme 1a), occurs rapidly to equilibrium state with K_4 (Scheme 1b), and only then the product slowly decomposes with the regeneration of PdP and oxidation in a two-electron redox process, which ends by releasing gaseous O_2.

Thus the ion-molecular mechanism of hydrogen peroxide decomposition was substantiated using chemical kinetics method. According to this mechanism, the only stable radicals involved in the reaction are the π radical cation forms of palladium(II) porphyrin catalysts.

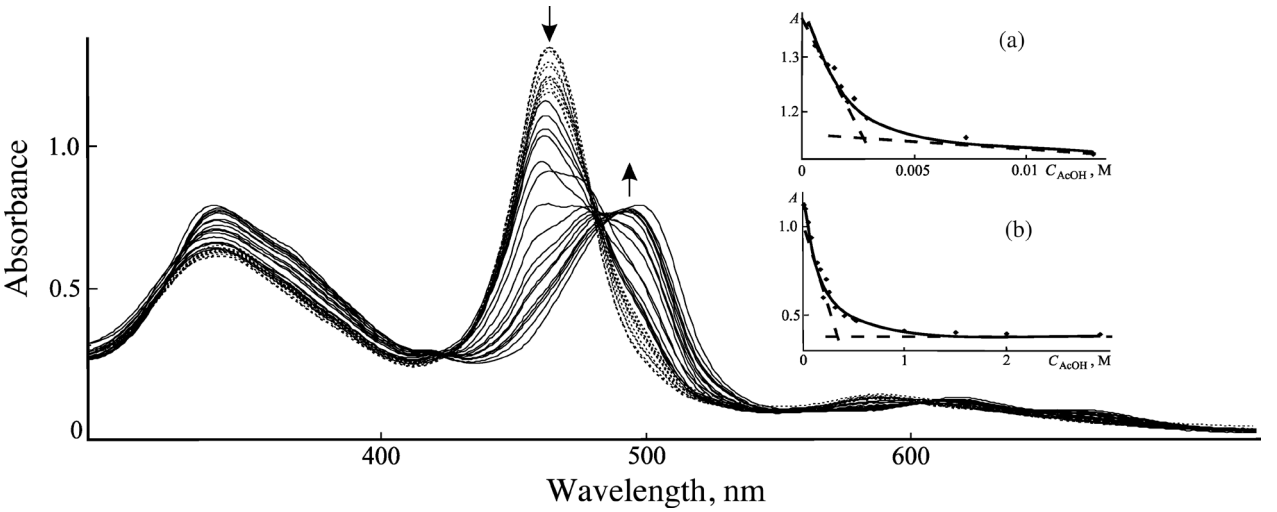

Fig. 8. Absorption spectra of $[O=ReTPP]_2O$ on addition of AcOH in benzene and curves of the spectrophotometric titration at λ_{max} = 461 nm; $C_{AcOH} = 2.92 \times 10^{-4}$–$1.30 \times 10^{-2}$ M (the broken lines and (a); $C_{AcOH} = 1.30 \times 10^{-2}$–2.92 M (the solid lines and (b), 298 K

The reversible dissociation of rhenium μ-oxo-dimer

The reaction of $[O=ReTPP]_2O$ in benzene-AcOH was studied at 298 K in wide AcOH concentration range (2.92×10^{-4}–2.92 M). It is shown that the presence of protons allows to reversible μ-oxo bridge destruction. The electronic absorption spectra of $[O=ReTPP]_2O$ in benzene in the presence of various amounts of AcOH and according spectrophotometric titration curves are shown in Fig. 8. Two spectral series changes are as the content of AcOH increases. These series with C_{AcOH} = 2.92×10^{-4}–1.30×10^{-2} M and $C_{AcOH} = 1.30 \times 10^{-2}$–2.92 M include:

— bands of increasing intensity with λ_{max} = 333 nm and bands of decreasing intensity with λ_{max} = 461 nm (Fig. 8,a);

— bands of increasing intensity with λ_{max} = 333 nm and batochromic displacement of band from 461 to 498 nm (Fig. 8,b).

These spectral results and the shape of the spectrophotometric titration curves show that the reaction occurs in two stages. The reversibility of these stages was substantiated by the study of changes in the electronic absorption spectrum as the concentration of AcOH decreased. The stoichiometry for the stepwise reactions was established using the curves of Equation (1) in a logarithmical form (Fig. 9).

At low AcOH concentrations the destruction of μ-oxo-bridge takes place and the equilibrium constant is $K_1 = (5.4 \pm 1.0) \times 10^2$ M^{-1}. It was found experimentally that the equilibrium at the first stage was established in approximately 5 min and characterized by the stoichiometry 1:1 (Fig. 9, line *1* ($\tan\alpha = 1.2$)). These data allow to the equation for the first reaction step in the form;

$$[O=ReTPP]_2O + AcOH \xleftrightarrow{K_1} O=Re(AcO)TPP + O=Re(OH)TPP \quad (33)$$

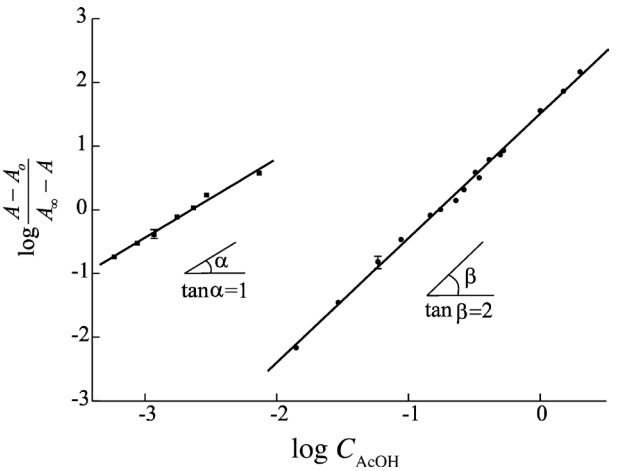

Fig. 9. Dependence of indicator ratio ($\log\frac{A_p-A_o}{A_\infty-A_p}$) on AcOH concentration ($\log C_{AcOH}$) for the reaction between $[O=ReTPP]_2O$ and AcOH in benzene at the (1) first and the (2) second stages. $R^2 = 0.99$

The second stage (34) of the reaction is observed at AcOH concentrations from 5.83×10^{-2} to 2.92 M and characterized by slow batochromic displacement of band from 461 to 498 nm. The equilibrium constant is $K_2 = (35 \pm 7)$ M^{-2}. Two AcOH molecules take part in the reaction (Fig. 9, line *2* ($\tan\beta = 1.9$)).

$$O=Re(AcO)TPP + O=Re(OH)TPP + 2AcOH \xleftrightarrow{K_2} O=Re(AcO)(AcOH)TPP + O=Re(AcO)(H_2O)TPP \quad (34)$$

It is obvious that constant K_2 represents a passing of the reactions in the first coordination sphere — coordination of AcOH by O=Re(AcO)TPP and O=Re(OH)TPP in the molecular and anion form

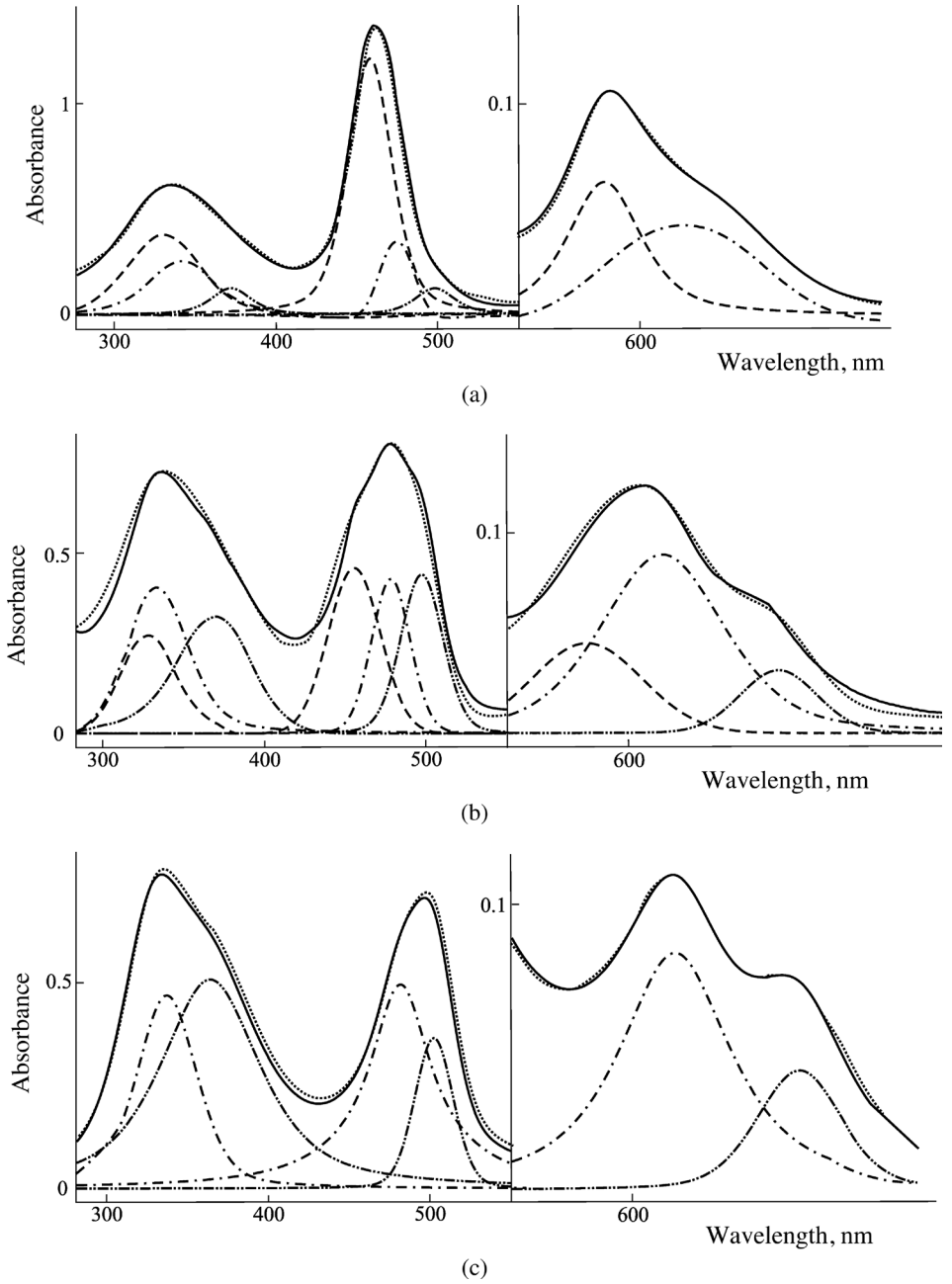

Fig. 10. Selected electronic spectra obtained during the titration of $[O=ReTPP]_2O$ with AcOH at 293 K. C_{AcOH}, M: (a) 2.92×10^{-4}, (b) 0.29, (c) 14.5. The broken lines show the calculated absorption based on the best fit

--------- $[O=ReTPP]_2O$; –·–·–· O=Re(OH)TPP; –··–··–·· O=Re(AcO)TPP. Absorption maxima are calculated using a Gaussian peak deconvolution

correspondently. The protonation of OH^- ligand takes place as well (34).

The composition of the coordination sphere of stepwise reaction products with AcOH was confirmed by the EAS (Fig. 10) and ^1H NMR methods. There is proton signal of OH^- at $\delta = -2.5$ [30] in ^1H NMR spectrum of $[O=ReTPP]_2O$ in intermediate area of acetic acid concentration (spectrum in $CDCl_3$ + 0.38 M AcOH). Those disappears in ^1H NMR spectrum of the final compound ($CDCl_3$ + 5 M AcOH) confirming OH^- ions are absent in the coordination sphere of complex. From EAS data (Fig. 10) it is important that the further increasing of AcOH concentration (3 M and above) does not change the compound EAS. The final spectrum by titration and the spectrum of $[O=ReTPP]_2O$ in 100% AcOH are analogies.

Only the ratio of kinetic coefficients of direct and return reactions can be obtained for the Re^v

complex transformations because of a fast equilibrium establishment. The study of the mechanism is not obviously possible without the kinetic description of reactions.

CONCLUSION

Thus an investigation with using of kinetic method allowed us to establish the stoicheometric mechanism of rhodium and palladium porphyrin complexes oxidation by aerated H_2SO_4 and mechanism of catalytic action of metal porphyrins in reaction of H_2O_2 decomposition. H-associated species of PdTPP, PdTetPOEP and (Cl)RhTPP were found to exist in sulfuric acid with concentrations of 16.33–17.38, 17.48–18.22 and 16.5–17.5 M, respectively. The kinetics of one-electron oxidation of complexes in the coordinated aromatic macrocycle was studied. A third-order rate equation was determined and the mechanism of the oxidation reaction was substantiated with kinetically significant stages of dioxygen coordination, electron transfer from the macrocyclic aromatic system to dioxygen, and H-association equilibrium between the complex and sulfuric acid.

The kinetics and spectral manifestations of alkaline decomposition of H_2O_2 in a water-dimethylformamide medium catalyzed by $Pd^{II}P$ was studied over a wide range of reagent concentrations under polythermal conditions. A complete kinetic description of the reacting systems was given, and the rates and set of elementary reactions, intermediate compounds, and kinetically significant equilibria were determined. All considered mechanisms of catalytic hydrogen peroxide decomposition reactions concern to an ion-molecular with respect to H_2O_2 and are realized through the stage of the formation of palladium(II) porphyrinate oxidized in the macrocycle.

The ratio of kinetic coefficients of direct and return reactions was obtained for the Re^{v} complex transformations in benzene–AcOH at 298 K in wide AcOH concentration range (2.92×10^{-4}–2.92 M). It is shown that the presence of protons allows to reversible μ-oxo bridge destruction. At low AcOH concentrations the destruction of μ-oxo-bridge takes place and the equilibrium constant is $K_1 = (5.4 \pm 1.0) \times 10^2$ M^{-1}. Coordination of AcOH by O=Re(AcO)TPP and O=Re(OH)TPP in the molecular and anion form correspondently ($K_2 = (35 \pm 7)$ M^{-2}) takes place at AcOH concentrations from 5.83×10^{-2}–2.92 M. The study of the mechanism is not obviously possible without the kinetic description of reactions.

Acknowledgements

We thank the Russian Foundation for Fundamental Research (Grant No. 09-03-97556), the N. 8 Program of Fundamental Research of Russian Academy of Science, Analytical Program RNP No. 2.2.1.1/2820 (2011), and The Federal Target Program "The scientific and scientific-pedagogical Staff of innovative Russia" (2009–2013, Action 1.1 - II turn).

REFERENCES

1. Meites L. *An Inrtoduction to Chemical Equilbrium and Kinetics*, Department of Chemistry Clarkson College of Technology, 1981; [L. Meites. *Vvedenie v kurs khimicheskoj termodinamiki I kineteki*. M.: Mir. 1984. 480 s. In Russian].
2. *Practical Chemical Kinetics. Chemical Kinetics in Problems with Decisions,* Melnikov M. (Ed.) Publishing house of the Moscow State University, Publishing house of the St.-Petersburg State University: 2006; pp 592.
3. Balieua S, Halimea Z, Lachkarb M and Boitrel B. *J. Porphyrins Phthalocyanines* 2008; **12**: 1223–1231.
4. Lebedeva AY, Troxlerb Th. and Vinogradov SA. *J. Porphyrins Phthalocyanines* 2008; **12**: 1261–1269.
5. Agboola BO, Mocheko A, Pillay J and Ozoemena KI. *J. Porphyrins Phthalocyanines* 2008; **12**: 1289–1299.
6. Kojima T, Nakanishi T, Honda T and Fukuzumi S. *J. Porphyrins Phthalocyanines* 2009; **13**: 14–21.
7. Ruiz GT, Lappin AG and Ferraudi G. *J. Porphyrins Phthalocyanines* 2010; **14**: 69–80.
8. Romeo A, Castriciano MA and Scolaro LM. *J. Porphyrins Phthalocyanines* 2010; **14**: 713–721.
9. Ghadamgahi M and Ajloo D. *J. Porphyrins Phthalocyanines* 2011; **15**: 240–256.
10. Valkova L, Borovkov N, Koifman O, Kutepov A, Berzina T, Fontana M, Rella R and Valli L. *Biosens. Bioelectron.* 2004; **20**: 1177–1184.
11. Bouvet M, Parrab V, Locatellib C and Xiongb H. *J. Porphyrins Phthalocyanines* 2009; **13**: 84–91.
12. Mandoj F, Nardis S, Pomarico G. and Paolesse R. *J. Porphyrins Phthalocyanines* 2008; **12**: 19–26.
13. Capar C, Thomas KE and Ghosh A. *J. Porphyrins Phthalocyanines* 2008; **12**: 964–967.
14. Tyulyaeva EYu, Kosareva OV, Klyueva ME and Lomova TN. *Zh. Neorg. Khim*. 2008; **53**: 1504–1509 [*Russ. J. Inorg. Chem.* 2008; **53**: 1405–1409].
15. Tipugina MYu and Lomova TN. *Zh. Neorg. Khim*. 2004; **49**: 1285–1291 [in Russian].
16. Suslova EE and Lomova TN. *Coord. Khim*. 2006; **32**: 163–173 [*Russ. J. Coord. Chem.* 2006; **32**: 155–165].
17. Lomova TN, Mozhzhykhina EG, Danilova EA and Islyaikin MK. *Zh. Phys. Khim.* 2009; **83**: 1877–1883 [*Rus. J. Phys. Chem.* 2009; **83**: 1694–1700].
18. Lomova TN, Shormanova LP and Berezin BD. *Zh. Neorg. Khim*. 1987; **32**: 2489–2492 [in Russian].
19. Semeikin AS. *Proceedings of XXIX Session of the Russian Workshop on the Chemistry of Porphyrins and Their Analogues,* Ivanovo, 2006; pp 19 [in Russian].
20. Lomova TN, Tyulyaeva EYu and Klyueva ME. In *Porphyrin Palladium(II) Complexes. Stable*

Intermediates in Some Redox and Catalytic Reactions. In Palladium: Compounds, Production and Applications, Brady KM. (Ed.) Nova Science Publishers, Inc.: New York, 2010; pp 285–306.
21. Lomova TN, Mozhzhukhina EG, Shormanova LP and Berezin BD. *Zh. Obshch. Khim.* 1989; **59**: 2317–2326 [in Russian].
22. Avlasevich YuS, Baluschev S, Jacob J, Muller K and Wegner G. *J. Porphyrins Phthalocyanines* 2006; **10**: 425.
23. Vinnik MI. *Uspehy Khim*. 1966; **35**: 1922–1952 [in Russian].
24. Lomova TN, Tyulyaeva EYu and Tipugina MYu. In *Advances in Porphyrin Chemistry,* Vol. 4, Golubchikov OA. (Ed.) St-Petersburg's State University: 2004; pp 147–160.
25. Tyulyaeva EYu, Lomova TN and Andrianova LG. *Zh. Neorg. Khim.* 2001; **46**: 432–437 [*Russ. J. Inorg. Chem.* 2001; **46**: 371].
26. Fialkov YuA. *The Solvent as Tool of Control of Chemical Process. Knowledge. New in a Life, a Science, Technics. A Series. "Chemistry"*, Vol. 6, 1988; pp 45.
27. Carnieri N and Harriman A. *Inorg. Chim. Acta*. 1982; **62**: 103–107.
28. Brown GH, Hopf FR, Meuer TJ and Whitten DG. *J. Am. Chem. Soc.* 1975; **97**: 5385–5390.
29. Deryabkina EV. *Candidate's Dissertation in Chemistry*, Ivanovo, 2001.
30. Collman JP, Barnes SE, Brothers PJ, Collins TJ, Ozava T, Galucci JC and Ibers JA. *J. Am. Chem. Soc.* 1984; **106**: 5151–5163.